Cancer Chemotherapy and Pharmacology (2019) 84:1303–1314
https://doi.org/10.1007/s00280-019-03965-5

ORIGINAL ARTICLE

NO donor inhibits proliferation and induces apoptosis by targeting PI3K/AKT/mTOR and MEK/ERK pathways in hepatocellular carcinoma cells

Ling Liu[1] · Jingjing Chen[1] · Mengyao Cao[1] · Jiangang Wang[1] · Shuying Wang[1]

Received: 28 May 2019 / Accepted: 16 September 2019 / Published online: 25 September 2019

Abstract

Background PABA/NO, O^2-{2,4-dinitro-5-[4-(*N*-methylamino) benzoyloxy] phenyl} 1-(*N*, *N*-dimethylamino) diazen-1-ium-1,2-diolate, is a diazeniumdiolate-based NO-donor prodrug that releases exogenous nitric oxide at high concentrations to induce apoptosis in many tumor cell lines.

Purpose This study aimed to determine the effects of PABA/NO on hepatocellular carcinoma proliferation and apoptosis induction both in vitro and in vivo experiments.

Results PABA/NO dramatically inhibited the growth of Bel-7402 hepatocellular carcinoma cells and significantly induced apoptosis in a concentration-dependent manner, accompanied by down-regulation of Bcl-2 and Bcl-xL, up-regulation of Bax and Bad, release of Cyt *c* and activation of cleaved-caspase-9/3 and cleaved-PARP, which were related to suppressing PI3K/AKT/mTOR and MEK/ERK signaling pathways. LY294002 (a PI3K inhibitor) and U0126 (an ERK inhibitor) prior to PABA/NO were found to synergistically enhance PABA/NO-induced apoptosis. Carboxy-PTIO as a NO scavenger obviously attenuated PABA/NO-induced apoptosis. Additionally, H22 tumor-bearing mice experiments demonstrated that PABA/NO exerted good anti-tumor effects via reducing tumor volume, tumor weight and decreasing the expression of CD34. Furthermore, PABA/NO treatment strongly inhibited the phosphorylation of PI3K/AKT/mTOR and MEK/ERK signaling pathways in H22 hepatocellular carcinoma tissues.

Conclusions PABA/NO induced apoptosis through inhibition of PI3K/Akt/mTOR and MEK/ERK pathway in hepatocellular carcinoma cells.

Keywords Nitric oxide · Apoptosis · PABA/NO · Hepatocellular carcinoma

Introduction

Human hepatocellular carcinoma (HCC) is a common malignancy in Eastern Asia and remains the fifth most commonly diagnosed malignancy around the world. Optimal treatments for HCC include cytotoxic chemotherapy, radiation treatment and surgery. However, effective treatment options for many patients with advanced hepatocellular carcinoma are restricted for various reasons [1, 2]. Some other factors that facilitate proliferation and restrain apoptosis could not be ignored in the long process of hepatocellular carcinoma development.

The phosphoinositide 3-kinase (PI3K)/AKT/mTOR and extracellular signal-regulated kinase (ERK) oncogenic signaling pathways are frequently hyperactivated in many cancer types, promoting cell proliferation and differentiation, deregulating control of metabolism, and increasing the progression of the disease [3, 4]. Both PI3K and ERK signaling pathways could be compensatory for each other when one of them is targeted by specific inhibitors, which result in activation of the other signaling pathway [5, 6]. Therefore, the initial therapeutic effects of targeting either pathway alone are diminished, which contributed to drug resistance. Co-inhibition of the PI3K/AKT/mTOR and MEK/ERK cascades has become keen pharmaceutical objectives. It is urgent to search for novel agents that targeting these two signaling pathways adequately [7, 8].

✉ Ling Liu
liuling921@126.com

[1] Department of Pharmacy, Medical College, Henan University of Science and Technology, 263 Kaiyuan Avenue, Luoyang 471023, China

Endogenous nitric oxide (NO) in cells is synthesized from L-arginine by nitric oxide synthetase (NOS). Macrophages and endothelial cells produce large amounts of endogenous NO through upregulating the activity of iNOS to kill tumor cells [9]. The half-life of exogenous NO in the body is relatively short and unstable in aqueous solution. NO donors can release NO through enzymatic action, prolong the half-life of NO and inhibit the growth of tumor cells, which are important tools for detecting the role of NO in cellular signal transduction processes [10]. Diazeniumdiolate (NONOates) has obvious advantages in the targeted release of NO [11, 12]. O^2-{2,4-dinitro-5-[4-(*N*-methylamino) benzoyloxy] phenyl} 1-(*N*, *N*-dimethylamino)diazen-1-ium-1,2-diolate (PABA/NO) is a diazeniumdiolate-based NO-donor prodrug [13, 14]. Specifically, PABA/NO reacts with intracellular glutathione (GSH) under GST catalysis to form a diazeniumdiolate anion that spontaneously releases NO. PABA/NO induces apoptosis and suppresses the proliferation of many tumor cells, such as breast cancer [15], promyelocytic leukemia [16], and hepatocellular carcinoma [17]. In our previous study, a novel PABA/NO-based oleanolic acid derivative induced human hepatoma cell apoptosis via a ROS/MAPK-dependent mitochondrial pathway [18]. However, the antitumor efficacy and molecular mechanisms of PABA/NO in vivo have not been further assessed and elucidated.

H22 mouse xenograft model is readily available for evaluating the anti-tumor effects in routine laboratory experiments [19]. In the present study, experiments were performed in vitro to demonstrate the inhibitory efficacy and molecular mechanisms of PABA/NO in H22 hepatocellular carcinoma. Our data demonstrated that PABA/NO inhibiting proliferation and inducing apoptosis of Bel-7402 hepatocellular carcinoma cells were associated with simultaneous inhibition of PI3K/AKT/mTOR and MEK/ERK. In vivo assays with H22 tumor-bearing mice verified the anti-tumor effects of PABA/NO with the abolition of PI3K/AKT/mTOR and MEK/ERK pathways. Together, these data indicate that PABA/NO could potentially improve the therapeutic outcome through the regulation of PI3K/AKT/mTOR and MEK/ERK pathways.

Materials and methods

PABA/NO was prepared as previously described [20] (Fig. 1a). It was dissolved in 100% DMSO to a concentration of 10 mM as a stock solution. The final concentration of DMSO did not exceed 0.1% throughout the study. Reagents were used in the present study including cell counting kit-8 (CCK-8) (Cat# CK04-1000T) (Dojindo Laboratories, Kumamoto, Japan), Annexin V-FITC/PI kit (Cat#556547) (BD Biosciences, NJ, San Diego, CA, USA) and DAPI staining solution (Beyotime, Haimen, China). The antibodies for Bax (Cat#5023), Bcl-2 (Cat#15071), Cytochrome C (Cat#11940), cleaved-caspase-3 (Cat#9664), cleaved caspase-9 (Cat#20750), phospho-PI3Kinase p85 (Tyr458)/p55 (Tyr199) (Cat#17366), p-Akt (Ser473) (Cat#4060), p-mTOR (Ser2448) (Cat#5536), p-70S6K (Cat# 9204), p-MEK1/2 (Ser217/221) (Cat#3958), p-p44/42 MAPK (ERK1/2) (Thr202/Tyr204) (Cat#4370), p-p90RSK (Ser380) (Cat#11989), LY294002 (Cat#9901) and U0126 (Cat#9903) were supplied by Cell Signaling Technology (Beverly, MA, USA). HRP-conjugated affinipure goat anti-mouse IgG (Cat# SA00001-1), HRP-conjugated affinipure goat anti-rabbit IgG (Cat# SA00001-2) and β-actin (Cat# 66009-1-Ig) were supplied by Proteintech Group, Inc (Wuhan, China). CD34 (Cat# BA0532) rabbit polyclonal antibody was purchased from Boster Biological Technology (Wuhan, China).

Cells culture

PLC5, Huh-7, Bel-7402, SMMC-7721 and HepG2 hepatocellular carcinoma cells were obtained from Chinese Academy of Sciences (Shanghai, China), cultured in RPMI 1640 medium (Gibco, Invitrogen Corporation, Carlsbad, CA, USA) supplemented with 10% FBS at 37 °C in a humidified atmosphere containing 5% CO_2.

Cell counting kti-8 (CCK-8) proliferation assays

Cells at a final density of 1.0×10^4 cells/well were seeded into 96-well cell plates overnight and incubated with various concentrations of PABA/NO for 24, 48 or 72 h. Thereafter, the medium with PABA/NO was removed and rapidly replaced with 100 μL medium containing 10μL CCK-8 reagent. After incubation at 37 °C for 2 h, the absorbance was measured using a spectrophotometer (Tecan, Switzerland) at a wavelength of 450 nm. Experiments were conducted in triplicate.

$$\text{Inhibition rate} = (\%) = \left[(\text{OD control} - \text{OD treated})/\text{OD control}\right] \times 100\%.$$

Annexin V-FITC/PI double staining assay

Cells were treated with different concentrations of PABA/NO for 24 h. Then, the cells were collected and resuspended in 500 μL binding buffer after treatment with PABA/NO. Five microliters of Annexin V-FITC and 5 μL PI were then added to these cells, which were kept in the dark for 10 min. The stained cells were analyzed by flow cytometry and calculated by Cell Quest software.

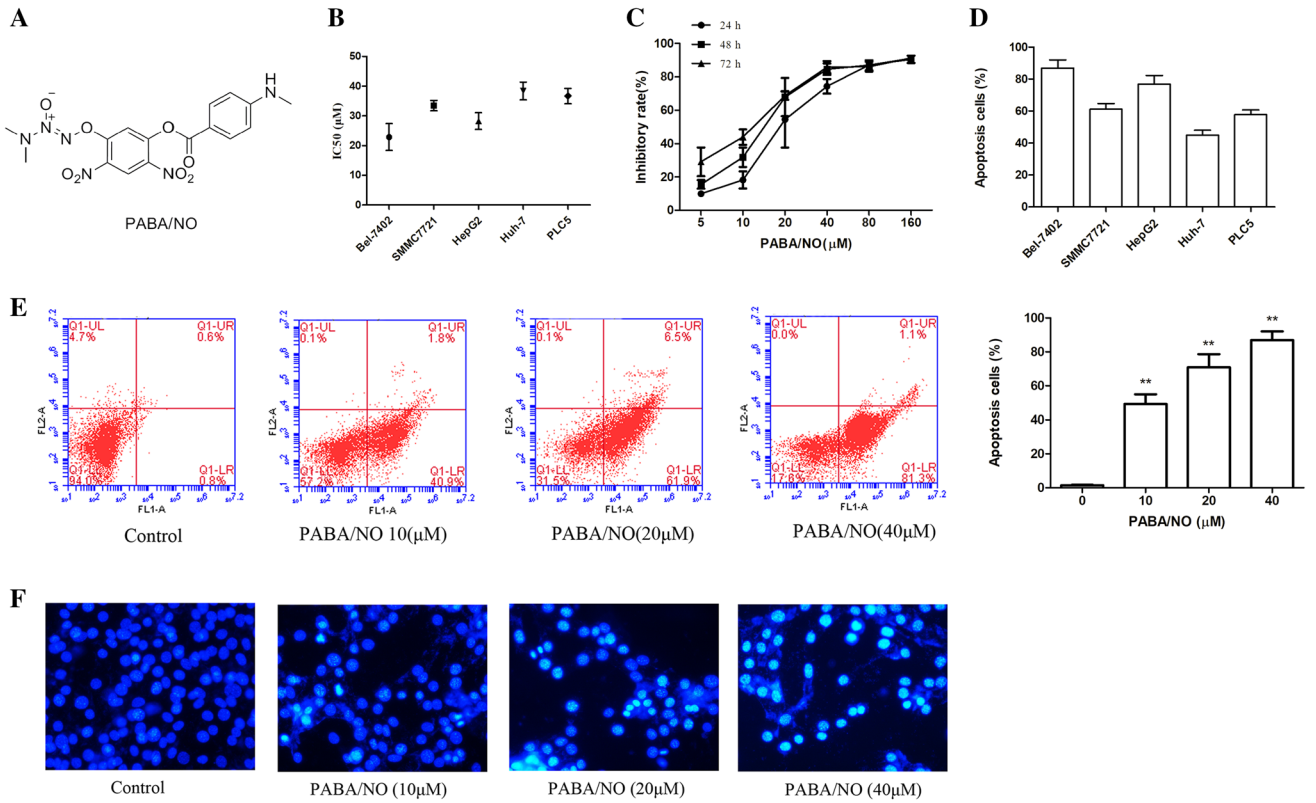

Fig. 1 Effects of PABA/NO on proliferation and apoptosis in hepatocellular carcinoma cells (HCC). **a** Chemical structure of PABA/NO. **b** Different half-growth inhibition concentration (IC50) of PABA/NO in the five HCC cells through CCK-8 assay. **c** Concentration- and time-dependent effects of PABA/NO on the growth of Bel-7402 cells. **d** Different apoptotic rates of PABA/NO in five HCC cells. The cells were treated with PABA/NO at 40 μM for 24 h and determined by the Annexin V-FITC/PI double staining assay. **e** Effects of PABA/NO on the apoptotic rate in Bel-7402 cells. The cells were treated with PABA/NO at different concentrations for 24 h and determined by the Annexin V-FITC/PI double staining assay. **f** Morphological observation under fluorescence microscopy after DAPI staining (×400 magnification). Data are mean ± SD. $n = 3$ for each concentration. $^{*}P < 0.05$, $^{**}P < 0.01$, vs. control group

DAPI staining assay

Cells were seeded into 6-well cell plate for 12 h and then treated with PABA/NO for 24 h. Then the cells were washed with PBS twice, and incubated with DAPI in accordance with the manufacturer's instructions. After staining, the cells were immediately observed by a fluorescence microscope (Olympus, IX-70, Japan).

Western blot analysis

The protein of total cell lysis was prepared according to the manufacturer's instructions. Protein was separated by sodium dodecyl sulfate polyacrylamide gel electrophoresis (SDS-PAGE) and transferred onto polyvinylidene difluoride membrane (PVDF, Millipore, USA). The membranes were blocked with 5% nonfat milk in TBS-T (Tris-buffered saline and 1% Tween 20) and incubated with primary antibodies at 4 °C overnight. The primary antibodies were used at 1:1000 dilution and beta-actin were used at 1:5000 dilution. HRP-conjugated goat anti-rabbit IgG or goat anti-mouse IgG were incubated for 2 h as the secondary antibodies. The secondary antibody was used at 1:10,000 dilution. Signals were visualized by Bio-Rad Universal Hood Gel Imaging System.

Animals

Male Balb/c mice, 20–22 g, acquired from Experimental Animal Center of Medical College in Henan University of Science and Technology (Luoyang, China), were acclimatized under standardized conditions (23 ± 2 °C, 60 ± 10% humidity, 12 h light/dark cycle) for 1 week prior to use. All experimental procedures were approved by and performed in accordance with the guidelines set out by the Institutional Animal Experiment Committee of Henan University of Science and Technology, China.

H22 transplanted model establishment

According to the established protocol (21, 22), H22 cells were subcutaneously injected the mice and grown for 7 days before implantation. The ivory white ascites were extracted from mice under sterile conditions. Normal saline was then added to adjust the tumor cell density to about 1×10^7 cells/mL. About 0.2 mL cell suspensions were then subcutaneously inoculated into the axillary region of the mice in all groups. Twenty-four male Balb/c mice were randomly divided into four groups with six mice in each group after transplantation. After the tumor reached 50–100 mm^3 following tumor cell injection, the control saline group and the PABA/NO (1 mg/kg, 2 mg/kg and 4 mg/kg) groups were all administered via tail vein injection every 3 days. Tumor size was measured every 2 days using a digital caliper and tumor volume was calculated using the formula: $V\ (mm^3) = W^2 \times L/2$, where W and L are the perpendicular smaller and larger diameters, respectively. The mice were treated with corresponding compounds daily for 14 days. At the end of the experiment, all mice were sacrificed and the tumors were segregated and weighed. Tumor inhibitory ratio was calculated by the following formula: $IR\ \% = (W_{Control} - W_{Treated})/W_{Control} \times 100\%$. $W_{Treated}$ and $W_{Control}$ were the tumor weight of the treated and control mice, respectively.

Histopathology and immunohistochemistry

At the end of the experiments, H22-transplanted tumor tissues were fixed overnight in 4% paraformaldehyde, embedded in paraffin, and sliced at 4 μm thickness for hematoxylin and eosin (H&E) and immunohistochemical staining. The sections were de-waxed in xylene, rehydrated through graded concentrations of ethanol and rinsed in PBS. Subsequently, endogenous peroxidase activity was quenched with 3% hydrogen peroxide for 20 min. To perform the necessary antigen retrieval, sections were submerged in citrate buffer (0.01 M, pH 6.0) at 95 °C for 20 min and incubated with bovine serum albumin for 1 h. Then the sections were washed in PBS for 3 min twice and the primary antibodies against CD34 (1:200), p-AKT (1:100) and p-ERK (1:100) were added at 4 °C overnight. The tissue was incubated at room temperature for 45 min. Sections were then washed and sequentially incubated with a secondary antibody at room temperature for 1 h, and then washed and colored with DAB staining and hematoxylin counter-staining. Brownish-yellow color in the cytoplasm of the cells was used to identify the expression of positive staining.

Statistical analysis

All results are expressed as the mean ± standard (SD). The data were analyzed using analysis of variance (ANOVA) to analyze the difference between groups. $P < 0.05$ was considered statistically significant.

Results

Effects of PABA/NO on cell proliferation in Bel-7402 cells

To determine whether PABA/NO has an inhibitory effect on the cell growth, PLC5, Huh-7, Bel-7402, SMMC-7721 and HepG2 hepatocellular carcinoma cells were exposed to different concentrations of PABA/NO (0, 5, 10, 20, 40, 80 or 160 μM) for 24 h. As shown in Fig. 1b, IC50 (50% inhibition of cell viability) values of PABA/NO for 24 h were 22.87 ± 4.53 μM (Bel-7402), 33.47 ± 1.41 (SMMC7721), 28.25 ± 2.32 (HepG2), 38.42 ± 2.47 (Huh-7), 36.68 ± 2.10(PLC5), which indicated PABA/NO exerted cytotoxicity in Bel-7402 cells more than other hepatocellular carcinoma cells. As shown in Fig. 1c, PABA/NO inhibited Bel-7402 cells viability in a dose- and time-dependent manner. IC50 values were 22.87 ± 4.53, 16.12 ± 1.13 and 11.20 ± 2.71 μM for 24, 48 and 72 h, respectively, indicating that PABA/NO inhibited the growth of Bel-7402 cells.

Effects of PABA/NO on cell apoptosis in Bel-7402 cells

To determine whether the cytotoxicity effects of PABA/NO against hepatocellular carcinoma cells resulted from apoptosis induction, Annexin V-FITC/PI staining assay was carried out. As shown in Fig. 1d, PABA/NO increased apoptosis rate significantly in Bel-7402 cells more than in other hepatocellular carcinoma cells for 24 h. These sensitive cells could reach approximate 90% apoptosis rate with PBAB/NO (40 μM) treatment. Furthermore, PABA/NO-treated cells significantly triggered apoptosis in a dose-dependent manner compared with untreated control ($P < 0.01$) (Fig. 1e). The proportions of apoptotic cells were 1.47 ± 0.21% (0 μM), 49.20 ± 5.75% (10 μM), 70.90 ± 7.76% (20 μM), 86.87 ± 5.15% (40 μM), respectively. Simultaneously, as depicted in Fig. 1e, cells in the control group displayed homogeneous fluorescence intensity in nucleus, while cells treated with PABA/NO displayed typical morphological change including condensed chromatin and fragmentation in the nucleus, which indicated that inhibitory effects of PABA/NO were associated with cell apoptosis.

Effects of PABA/NO on the expression of apoptosis-related protein in Bel-7402 cells

Next, the signaling pathways related to apoptosis induction were explored in PABA/NO-treated cells. The results

showed that exposure to PABA/NO could decrease the expression of Bcl-2 and Bcl-xL but also increase the expression of Bax and Bad (Fig. 2a, b). Simultaneously, Cyt *c* release from mitochondria to cytosol significantly caused activation of cleaved-caspase-9, cleaved-caspase-3 and cleavage of PARP, which corroborated the significant inhibitory effects of PABA/NO via inducing cell apoptosis.

Effects of PABA/NO on PI3K/AKT/mTOR and MEK/ERK signaling pathways in Bel-7402 cells

To further evaluate whether the effects of PABA/NO on apoptosis were related to PI3K/AKT/mTOR and MEK/ERK axes, two significant proliferative-related signaling pathways were observed. As shown in Fig. 2c, d, the results showed that PABA/NO treatment strongly inhibited the phosphorylation of MEK compared with the control group. Similarly, the phosphorylation levels of ERK, and p90RSK were also effectively attenuated by PABA/NO treatment. In addition, PABA/NO could remarkably restrain phosphorylation of PI3K, AKT, mTOR and R70S6K.

To further confirm that apoptosis caused by PABA/NO was linked with PI3K and ERK kinase signaling pathways, cells were pretreated with ERK inhibitor (U0126) and PI3K inhibitor (LY294002) for 2 h, respectively. As shown in Fig. 3a, both inhibitors could increase the effects of PABA/NO on the down-regulation of Bcl-2, up-regulation of Bax and activation of cleaved-caspase-3. Accordingly, the concurrent treatment with U0126 markedly enhanced the phosphorylation inhibition of MEK, ERK1/2 and p90RSK in PABA/NO-treated cells (Fig. 3b). Meanwhile, the phosphorylation inhibition of PI3K, AKT, mTOR and R70S6K were strengthened by LY294002 in PABA/NO-treated Bel-7402 cells (Fig. 2c). These results indicated that PABA/NO inhibited PI3K/AKT/mTOR and MEK/ERK pathways in hepatocellular carcinoma cells.

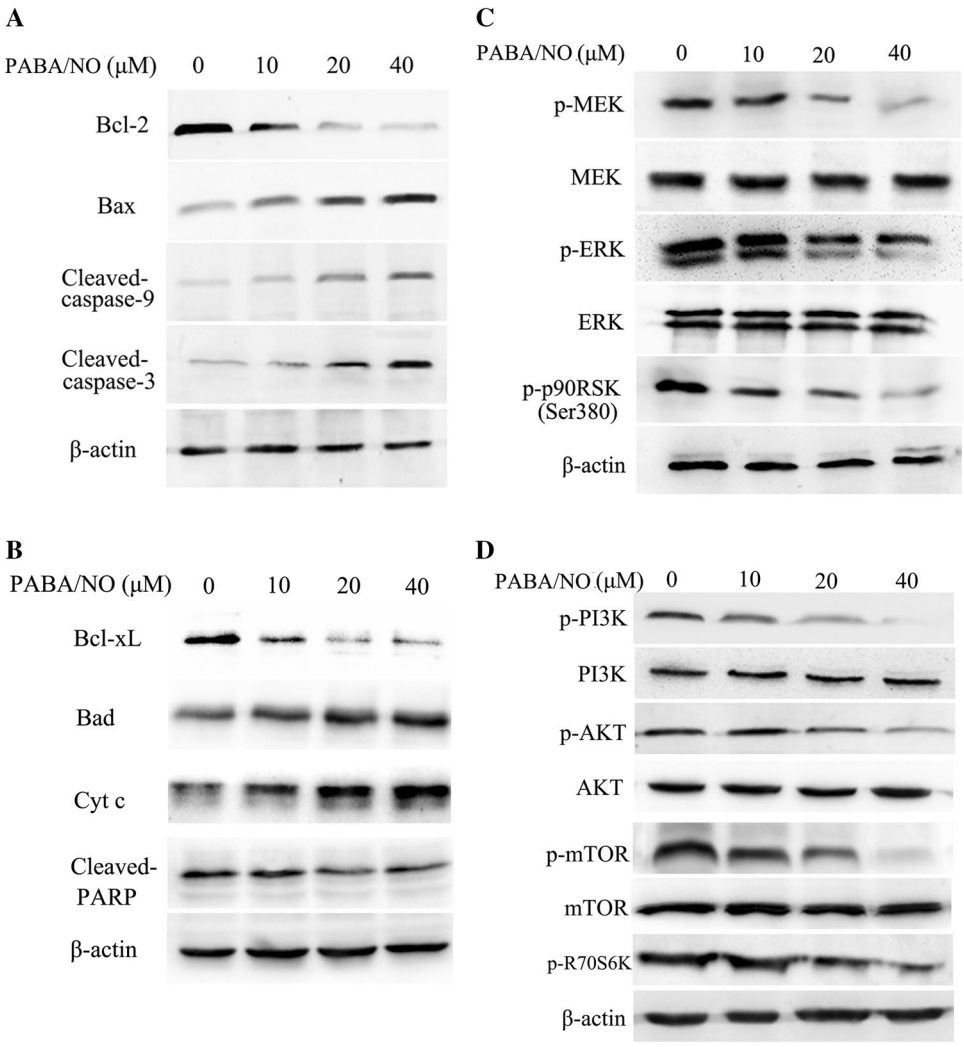

Fig. 2 Effects of PABA/NO on the expressions of caspase cascade, PI3K/AKT/mTOR and MEK/ERK pathways-related proteins in hepatocellular carcinoma cells. **a**, **b** Effects of PABA/NO on the expression of apoptotic-related proteins. **c** Effects of PABA/NO on the expression of MEK/ERK pathway-related proteins. **d** Effects of PABA/NO on the expression of PI3K/AKT/mTOR pathway-related proteins

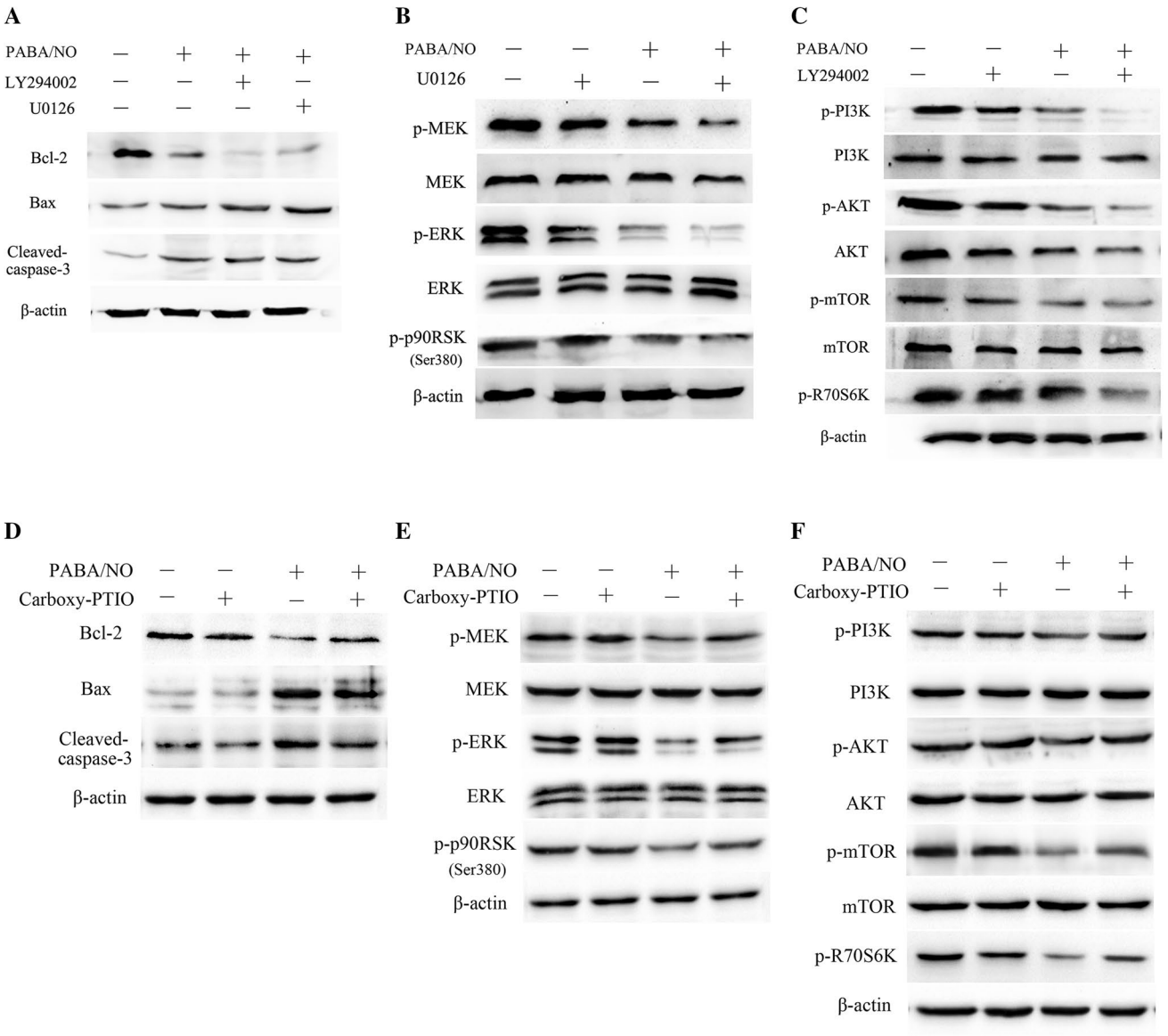

Fig. 3 Effects of LY294002, U0126 and Carboxy-PTIO on PABA/NO-induced cell apoptosis. **a** Effect of LY294002 and U0126 treatment as a specific inhibitor on the expression of apoptotic-related proteins. **b** Effect of U0126 treatment on the expression of MEK/ERK pathway-related proteins. **c** Effect of LY294002 on the expressions of PI3K/AKT/mTOR pathway-related proteins. The cells were pretreated with LY294002 (10 μM) or U0126 (10 μM) for 2 h, and then stimulated with PABA/NO (20 μM) for 24 h. **d** Effect of Carboxy-PTIO on the expression of apoptotic-related protein. The cells were pretreated with Carboxy-PTIO (50 μM) and then stimulated with PABA/NO (20 μM) for 24 h. **e** Effect of Carboxy-PTIO treatment on the expression of MEK/ERK pathway-related proteins. **f** Effect of Carboxy-PTIO treatment on the expressions of PI3K/AKT/mTOR pathway-related proteins. The expressions of protein were assessed by Western blotting analysis. Data are mean ± SD ($n = 3$) for each concentration

Effects of carboxy-PTIO on PABA/NO-induced cell apoptosis

To further confirm whether NO released from PABA/NO was related to PI3K/AKT/mTOR and MEK/ERK axes, effects of Carboxy-PTIO as a NO scavenger on PABA/NO-treated Bel-7402 cells were observed. As shown in Fig. 3d, Carboxy-PTIO as a NO scavenger obviously attenuated the PABA/NO-induced down-regulation of Bcl-2, up-regulation of Bax, and cleaved-caspase-3, which demonstrated that PABA/NO induced cell apoptosis via NO release. Simultaneously, pre-treatment with Carboxy-PTIO remarkably abolished PABA/NO-induced inhibitory effects on PI3K/AKT/mTOR and MEK/ERK pathways. Carboxy-PTIO canceled the effects of PABA/NO on down-regulation of phosphorylated MEK and ERK, which accordingly resulted in decrease of phosphorylated p90RSK (Fig. 3e). Meanwhile, down-regulation of phosphorylated effects on PI3K, AKT, mTOR

and R70S6K were attenuated by Carboxy-PTIO in PABA/NO-treated Bel-7402 cells (Fig. 3f). These data indicated the correlation between PABA/NO-induced apoptosis and two signaling pathways.

Effects of PABA/NO on tumor growth in H22 tumor-bearing mice

To further confirm the anti-tumor activity of PABA/NO in vivo, a murine H22 hepatocarcinoma model was established. As shown in Fig. 4A, PABA/NO significantly decreased tumor volume as compared with the control group after the 14-day treatments. Meanwhile, PABA/NO exerted evident inhibitory effects through the decrease in tumor weight. The average tumor weight in control group was 1.60 ± 0.13 g, while the tumor weights in PABA/NO-treated groups (1, 2, 4 mg/kg) obviously decreased to 1.18 ± 0.12, 0.87 ± 0.14 and 0.62 ± 0.13 g, respectively ($P > 0.01$), and the inhibitory rates of 25.94%, 45.78% and 60.89%, respectively. The average weight of tumors in PABA/NO-treated mice was significantly lower than in control mice (Fig. 4b, c). Furthermore, PABA/NO had little effect on the body weights of treated mice (Fig. 4d).

To further verify the anti-tumor effects of PABA/NO, tumor samples were determined following routine H&E staining. As shown in Fig. 3e, tumor cells in H22-transplanted group were tightly aligned, having a large blue-hued nucleus and clearly apparent nucleolus. However, tumor cells in PABA/NO-treated groups were characterized by arranged loosely, cytoplasm condenses, nuclear fragmentation, and the presence of large areas of apoptosis and necrotic region. All the data implied that PABA/NO exerted evident inhibitory effects on tumor growth in H22 tumor-bearing mice.

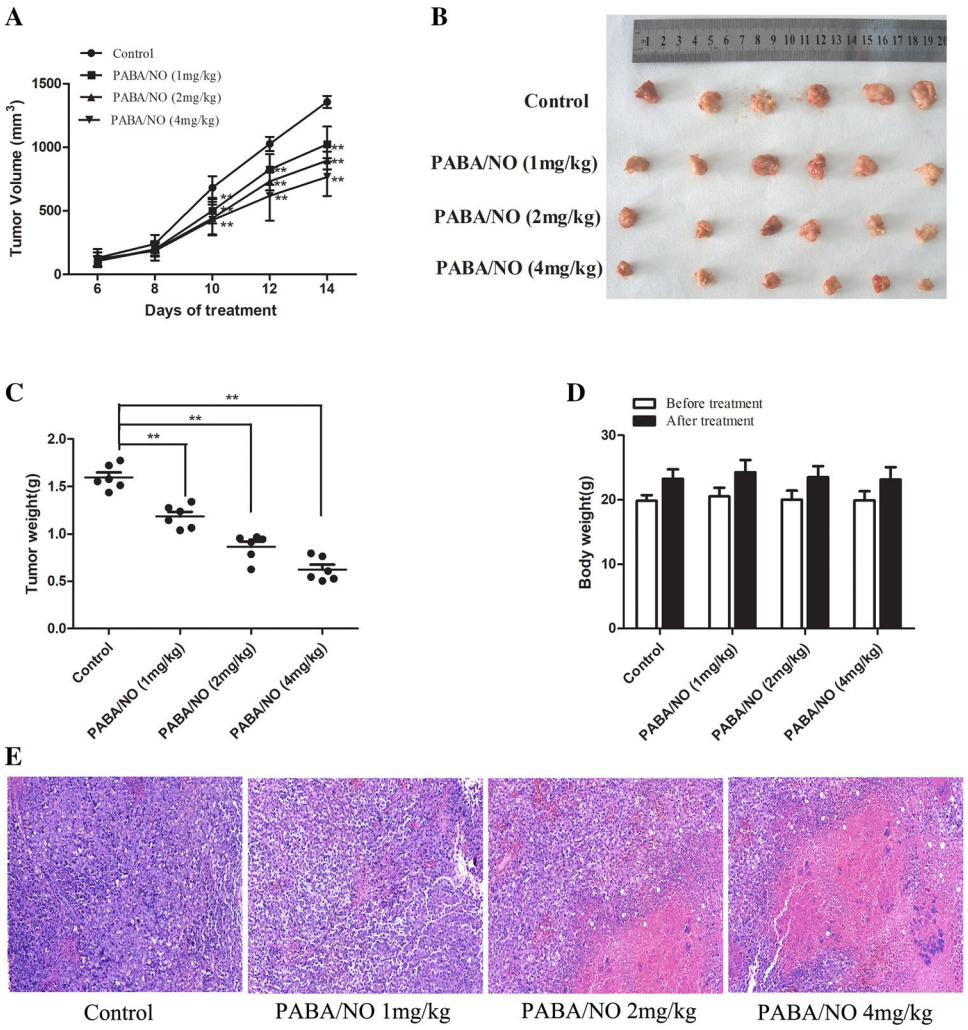

Fig. 4 Effects of PABA/NO on tumor growth in H22 tumor-bearing mice. **a** Effect of PABA/NO on H22 tumor volumes. **b** Gross picture of tumor-bearing mice in control and treated mice. **c** Effect of PABA/NO on tumor weights in control and treated mice. **d** Effect of PABA/NO on the body weights of tumor-bearing mice. **e** Morphological observation under microscopy after HE staining (×100 magnification). Data are expressed as the mean ± SD ($n = 6$). *$P < 0.05$, **$P < 0.01$ versus control group

Effects of PABA/NO on tumor-related angiogenesis in H22 tumor-bearing mice

We also choose vascular endothelial cells as our target to explore whether the antiangiogenic effect was caused by PABA/NO. Immunostaining with antibodies against CD34 special marker for endothelial cells was applied and cells positive were stained brown (Fig. 5a). The expression of CD34 in PABA/NO treatment group was obviously lower than that in control group. The results showed that PABA/NO displayed inhibition of microvessel density (MVD) in comparison to the control group at a different concentration ($P < 0.05$), which suggests that PABA/NO inhibits angiogenesis in H22 tumor-bearing mice.

Effects of PABA/NO on PI3K/AKT/mTOR and MEK/ERK signaling pathways in H22 tumor-bearing mice

Based on immunohistochemical staining, p-AKT and p-ERK were expressed in the cytoplasm of tumor cells (Fig. 5b, c). Cells positive for PI3K and p-ERK were stained brown as the arrow shows. Expressions of PI3K and p-ERK in the control group were markedly higher than that in PABA/NO-treated groups.

To further explore whether its effect on both signaling pathways is related to cell apoptosis, we detected the expression of protein involving two signaling pathways in tumor tissue. As shown in Fig. 5d, protein expression of the phosphorylation levels of AKT, mTOR, and p70S6K

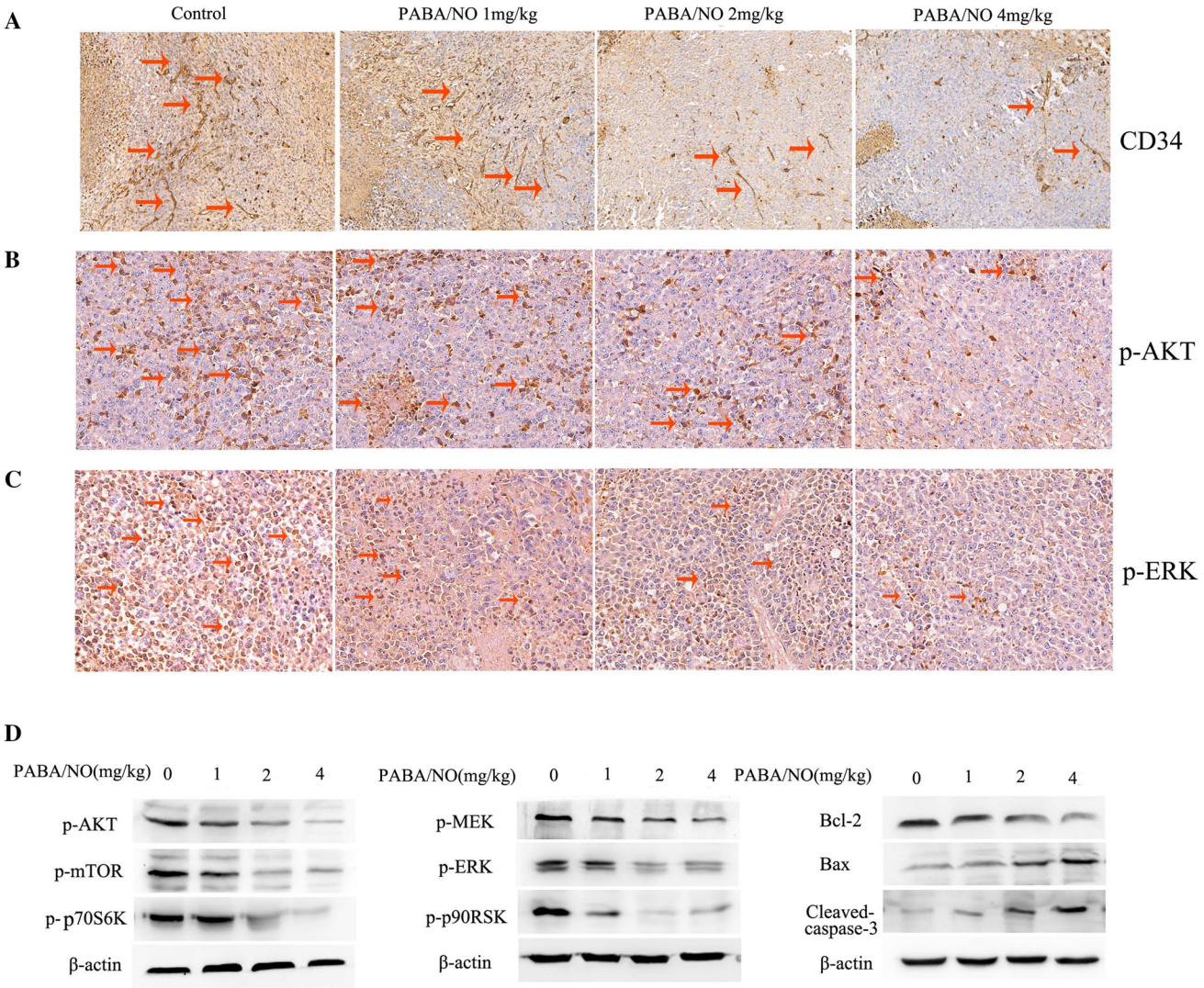

Fig. 5 Effects of PABA/NO on PI3K/AKT/mTOR and MEK/ERK signaling pathways in H22 tumor-bearing mice. **a** Effects of PABA/NO on tumor-related angiogenesis. **b** Immunohistochemical staining of p-AKT in H22 liver tumor tissues (IHC, ×200 magnification). **c** Immunohistochemical staining of p-ERK in H22 liver tumor tissues (IHC, ×100 magnification). **d** Effects of PABA/NO on the expressions of caspase cascade, PI3K/AKT/mTOR and MEK/ERK pathways-related proteins

were effectively attenuated following PABA/NO treatment. Similarly, PABA/NO could remarkably restrain phosphorylation of MEK, ERK and p90RSK, especially at the concentration of 2 mg/kg and 4 mg/kg. The results also showed that PABA/NO at each concentration could decrease the expression of Bcl-2 but also increase the expression of Bax. Activity of cleaved-caspase-3 was up-regulated. The results suggested that PABA/NO treatment strongly inhibited the phosphorylation of PI3K/AKT/mTOR and MEK/ERK signaling pathways, which resulted in the apoptosis of hepatoma H22-bearing mice.

Discussion

It is widely recognized that PI3K/AKT/mTOR and MEK/ERK pathways play modulating effects on the cellular processes including survival, proliferation, migration, and invasion, which cause cell damage and physiological dysfunctions [21, 22]. PABA/NO as a novel nitric oxide prodrug was involved in multiple events in cancer, including cell apoptosis, angiogenesis, and metastasis, and chemosensitization [23, 24]. In the present study, we demonstrated that PABA/NO could induce apoptosis in hepatocellular carcinoma cells, especially in Bel-7402 cells and have evidently inhibitory effects on tumor growth in H22 tumor-bearing mice.

Uncontrolled tumor cells that spread to other sites and escape from apoptosis play a critical role in carcinoma growth. Therefore, the inhibitions of cancer proliferation and apoptosis induction have been regarded as a crucial target for cancer treatment. In the present study, hepatocellular carcinoma cells' growth was suppressed and cell apoptosis was caused with the concentration of PABA/NO increased. The cells showed a significant externalization of phosphatidylserine, formation of apoptotic bodies and condensation of nuclear chromatin after DAPI staining.

Bcl-2 family proteins have been associated with mitochondrial dysfunction, leakage of cytochrome c, and downstream apoptotic activation. We observed a direct modulation of Bcl-2 family proteins level during PABA/NO-induced apoptosis. Total cell expression of pro-apoptotic Bcl-2 family proteins Bax and Bak was differentially increased in Bel-7402 cells compared to Bcl-2 and Bcl-xL levels. Other studies have indicated that the increase in pro-apoptotic proteins Bax with decreased levels of anti-apoptotic proteins like Bcl-2 in both total and mitochondrial fractions are a major driving force in mitochondrial dysfunction and subsequent apoptosis in some anti-cancer treatments [25]. Our data further support these observations as PABA/NO regulated Bcl-2 family protein levels that could lead to the increase of cytosolic cytochrome c levels, and apoptosis. In addition, the members of the caspase family of cysteine proteases are important mediators involved in apoptosis. The results demonstrated that caspase-9 and caspase-3 were activated in Bel-7402 cells following exposure to PABA/NO, which subsequently activates PARP that is associated with apoptosis.

Evidently, PABA/NO could evidently induce apoptosis in Bel-7402 cells. Moreover, a murine H22 tumor model was established to better evaluate the anti-tumor efficacy of PABA/NO in vivo. Consistent with the results in vitro, PABA/NO exerted evident inhibitory effects through decreasing tumor weight and tumor volume as compared with the control group. The favorable anti-tumor efficacy makes PABA/NO a potential NO donor for the treatment of cancer.

Both PI3K/AKT/mTOR and MEK/ERK signaling pathways are frequently hyperactivated or dysregulated in a large proportion of human cancers, which are crucial survival-related signaling pathways and were activated by diverse growth factors. Targeting these signaling pathways could supply a very promising approach for treating cancer therapy [22]. AKT is one of the major substrates and signaling mediators of PI3K, which is activated by phosphorylation within the carboxy terminus at Ser473 [26, 27]. This phosphorylation event in turn coordinates cell growth, survival, glycolysis, cell migration and invasion. Actually, aberrant activation of AKT signaling is generally involved in the pathogenesis of cancer and contributes to a poor outcome. AKT also plays a critical role in cell growth by directly phosphorylating mTOR at Ser2448, which responds to a phosphatidic acid-mediated signal to transmit a positive signal to p70 S6 kinase [28, 29]. Phosphorylation of p70 S6 kinase is required for cell growth. These events result in the translation of specific mRNA subpopulations to mediate cell survival, cell apoptosis and its activation increases with progression of the disease. In the present study, we found that PABA/NO attenuated the PI3K/AKT/mTOR pathway through decrease in phosphorylation of PI3K p85 at Tyr458, AKT at Ser473, mTOR at Ser2448 and p70S6 K at Thr389 in PABA/NO-treated Bel-7402 cells. In addition, LY294002 as a specific PI3Kinase inhibitor can aggravate PABA/NO-induced apoptosis. Accordingly, the inactivation of PI3K/AKT/mTOR signaling pathway was also observed in H22 tumor-bearing mice with the treatment of PABA/NO. These results suggested the inactivation of PI3K/AKT/mTOR pathway should play a main role in PABA/NO-induced apoptosis. The inactivation of this pathway can directly decrease phosphorylation of transcription factors that resulted in decreased expression of anti-apoptotic members of the Bcl-2 family and increased levels of pro-apoptotic proteins, thus activating the caspase-3 apoptotic cascade.

Generally, crosstalk between the PI3K/AKT/mTOR and MEK/ERK pathways is abnormally regulated in tumors. Consequently, the dysregulations of PI3K/AKT/mTOR pathway lead to a compensatory activation of the MEK/

ERK signaling pathway [30, 31]. MEK is a dual-specificity protein kinase that functions in a mitogen-activated protein kinase cascade controlling cell growth and differentiation. MEK activates p44 and p42 MAP kinase (ERK1/2) by phosphorylating both threonine and tyrosine residues at sites located within the activation loop of kinase subdomain VIII [32]. The p90 ribosomal S6 kinases (RSKs) comprise a family of serine/threonine kinases that are downstream effectors of the ERK pathway [33]. The activation of RSK plays an active role in nuclear signaling by phosphorylating several substrates including c-Fos, IκB and Bad to protect cells from apoptosis [34]. In the present study, we found that PABA/NO repressed the MEK/ERK pathway through decreased phosphorylation of MEK at Ser217/221, ERK at Thr202/Tyr204, and p90RSK at Ser380 in PABA/NO-treated Bel-7402 cells. ERK inhibitor U0126 could greatly intensify the apoptotic effects on PABA/NO-treated Bel-7402 cells compared to PABA/NO single treatment. Pre-treatment of Carboxy-PTIO further supported the correlation between PABA/NO-induced apoptosis and two signaling pathways. The same results were observed in H22 tumor-bearing mice with the treatment of PABA/NO. The phosphorylation of ERK is activated in hepatoma H22-bearing mice tissues while PABA/NO could decrease it and its substrates, which indicated the suppression of MEK/ERK pathway is essential for PABA/NO-induced caspase-3 apoptotic cascade. The new blood vessels formation may be expressed using markers expressed by endothelial cells such as CD31, CD34, and CD105 [35]. Microvascular density (MVD) may be assessed based on immunohistochemical techniques and also may be used as prognostic indicator for the increase in metastatic risk. Immunohistochemistry studies on CD34 immunolabelled tumors demonstrated that the MVD of CD34 positive blood vessels is linked with cancer progression and prognosis [36]. A higher number of CD34-positive blood vessels is inversely related to survival. PI3K inhibition modulates the tumor vasculature, either directly (by inhibiting endothelial cells) or indirectly (by inhibiting angiogenesis-promoting tumor-associated myeloid cells and VEGF production by tumor cells) [37]. The vascular responses to PI3K inhibitors can be attributed to effects on both the endothelial cells and the tumor cells, and the crosstalk between them, for example, by dampening the production of VEGF by the tumor cells, with differences observed depending on the tumor model used [38]. Both angiogenesis and signaling through the RAF/mitogen-activated protein (MAP)/extracellular signal-regulated kinase (ERK) kinase (MEK)/ERK (RAF/MEK/ERK) cascade play critical roles in the development of tumor cells. The anti-tumor activity of agents may be attributed to inhibition of tumor angiogenesis and direct effects on tumor cell proliferation/survival [39]. PABA/NO displayed inhibition of microvessel density which might be attributed to inhibitory effects on the PI3K/AKT/mTOR and MEK/ERK signaling pathways in hepatoma H22-bearing mice tissues.

Conclusively, PABA/NO could inhibit proliferation and induce apoptosis both in Bel-7402 carcinoma cells and in hepatoma H22-bearing mice via suppressing the PI3K/AKT/mTOR and MEK/ERK signaling pathways. Therefore, the present study might provide fundamental knowledge for understanding the anti-tumor activity of PABA/NO in hepatocellular carcinoma cells.

Funding This study was funded by the National Natural Science Foundation of China (No. 81502627) and the Young Backbone Teachers Assistance Scheme of Henan Province Colleges and Universities (No. 2016GGJS-065).

Compliance with ethical standards

Conflict of interest All authors declare that they have no conflict of interest.

Ethical approval All applicable international, national, and/or institutional guidelines for the care and use of animals were followed.

References

1. Ikeda M, Morizane C, Ueno M, Okusaka T, Ishii H, Furuse J (2018) Chemotherapy for hepatocellular carcinoma: current status and future perspectives. Jpn J Clin Oncol 48(2):103–114. https://doi.org/10.1093/jjco/hyx180
2. Moriguchi M, Umemura A, Itoh Y (2016) Current status and future prospects of chemotherapy for advanced hepatocellular carcinoma. Clin J Gastroenterol 9(4):184–190. https://doi.org/10.1007/s12328-016-0670-7
3. Roof AK, Gutierrez-Hartmann A (2018) Consider the context: Ras/ERK and PI3K/AKT/mTOR signaling outcomes are pituitary cell type-specific. Mol Cell Endocrinol 463:87–96. https://doi.org/10.1016/j.mce.2017.04.019
4. Ye C, Yu X, Liu X, Dai M, Zhang B (2018) miR-30d inhibits cell biological progression of Ewing's sarcoma by suppressing the MEK/ERK and PI3K/Akt pathways in vitro. Oncol Lett 15(4):4390–4396. https://doi.org/10.3892/ol.2018.7900
5. Asati V, Mahapatra DK, Bharti SK (2016) PI3K/Akt/mTOR and Ras/Raf/MEK/ERK signaling pathways inhibitors as anticancer agents: structural and pharmacological perspectives. Eur J Med Chem 109:314–341. https://doi.org/10.1016/j.ejmech.2016.01.012
6. Jokinen E, Koivunen JP (2015) MEK and PI3K inhibition in solid tumors: rationale and evidence to date. Ther Adv Med Oncol 7(3):170–180. https://doi.org/10.1177/1758834015571111
7. Zhou J, Zhao T, Ma L, Liang M, Guo YJ, Zhao LM (2017) Cucurbitacin B and SCH772984 exhibit synergistic anti-pancreatic cancer activities by suppressing EGFR, PI3K/Akt/mTOR, STAT3 and ERK signaling. Oncotarget 8(61):103167–103181. https://doi.org/10.18632/oncotarget.21704
8. Zhu J, Yao J, Huang R, Wang Y, Jia M, Huang Y (2018) Ghrelin promotes human non-small cell lung cancer A549 cell proliferation through PI3K/Akt/mTOR/P70S6 K and ERK signaling pathways. Biochem Biophys Res Commun 498(3):616–620. https://doi.org/10.1016/j.bbrc.2018.03.031

9. Yasuda H (2008) Solid tumor physiology and hypoxia-induced chemo/radio-resistance: novel strategy for cancer therapy: nitric oxide donor as a therapeutic enhancer. Nitric Oxide 19(2):205–216. https://doi.org/10.1016/j.niox.2008.04.026
10. Maher A, Abdel Rahman MF, Gad MZ (2017) The role of nitric oxide from neurological disease to cancer. Adv Exp Med Biol 1007:71–88. https://doi.org/10.1007/978-3-319-60733-7_5
11. Huang Z, Fu J, Zhang Y (2017) Nitric oxide donor-based cancer therapy: advances and prospects. J Med Chem 60(18):7617–7635. https://doi.org/10.1021/acs.jmedchem.6b01672
12. Kang F, Ai Y, Zhang Y, Huang Z (2018) Design and synthesis of new hybrids from 2-cyano-3,12-dioxooleana-9-dien-28-oic acid and O(2)-(2,4-dinitrophenyl) diazeniumdiolate for intervention of drug-resistant lung cancer. Eur J Med Chem 149:269–280. https://doi.org/10.1016/j.ejmech.2018.02.062
13. Findlay VJ, Townsend DM, Saavedra JE, Buzard GS, Citro ML, Keefer LK, Ji X, Tew KD (2004) Tumor cell responses to a novel glutathione S-transferase-activated nitric oxide-releasing prodrug. Mol Pharmacol 65(5):1070–1079. https://doi.org/10.1124/mol.65.5.1070
14. Townsend DM, Findlay VJ, Fazilev F, Ogle M, Fraser J, Saavedra JE, Ji X, Keefer LK, Tew KD (2006) A glutathione S-transferase pi-activated prodrug causes kinase activation concurrent with S-glutathionylation of proteins. Mol Pharmacol 69(2):501–508. https://doi.org/10.1124/mol.105.018523
15. Xiong Y, Manevich Y, Tew KD, Townsend DM (2012) S-Glutathionylation of protein disulfide isomerase regulates estrogen receptor alpha stability and function. Int J Cell Biol 2012:273549. https://doi.org/10.1155/2012/273549
16. Hutchens S, Manevich Y, He L, Tew KD, Townsend DM (2011) Cellular resistance to a nitric oxide releasing glutathione S-transferase P-activated prodrug, PABA/NO. Invest New Drugs 29(5):719–729. https://doi.org/10.1007/s10637-010-9407-5
17. Fu J, Liu L, Huang Z, Lai Y, Ji H, Peng S, Tian J, Zhang Y (2013) Hybrid molecule from O2-(2,4-dinitrophenyl)diazeniumdiolate and oleanolic acid: a glutathione S-transferase pi-activated nitric oxide prodrug with selective anti-human hepatocellular carcinoma activity and improved stability. J Med Chem 56(11):4641–4655. https://doi.org/10.1021/jm400393u
18. Liu L, Fu J, Li T, Cui R, Ling J, Yu X, Ji H, Zhang Y (2012) NG, a novel PABA/NO-based oleanolic acid derivative, induces human hepatoma cell apoptosis via a ROS/MAPK-dependent mitochondrial pathway. Eur J Pharmacol 691(1–3):61–68. https://doi.org/10.1016/j.ejphar.2012.07.031
19. Sun S, Ji H, Feng Y, Kang Y, Yu J, Liu A (2018) A novel mechanism of tumor-induced thymic atrophy in mice bearing H22 hepatocellular carcinoma. Cancer Manag Res 10:417–424. https://doi.org/10.2147/CMAR.S157512
20. Ji X, Pal A, Kalathur R, Hu X, Gu Y, Saavedra JE, Buzard GS, Srinivasan A, Keefer LK, Singh SV (2008) Structure-based design of anticancer prodrug PABA/NO. Drug Des Dev Ther 2:123–130
21. Cui SX, Shi WN, Song ZY, Wang SQ, Yu XF, Gao ZH, Qu XJ (2016) Des-gamma-carboxy prothrombin antagonizes the effects of sorafenib on human hepatocellular carcinoma through activation of the Raf/MEK/ERK and PI3K/Akt/mTOR signaling pathways. Oncotarget 7(24):36767–36782. https://doi.org/10.18632/oncotarget.9168
22. Wu YL, Maachani UB, Schweitzer M, Singh R, Wang M, Chang R, Souweidane MM (2017) Dual inhibition of PI3K/AKT and MEK/ERK pathways induces synergistic antitumor effects in diffuse intrinsic pontine glioma cells. Transl Oncol 10(2):221–228. https://doi.org/10.1016/j.tranon.2016.12.008
23. Kim Y, Maciag AE, Cao Z, Deschamps JR, Saavedra JE, Keefer LK, Holland RJ (2015) PABA/NO lead optimization: improved targeting of cytotoxicity to glutathione S-transferase P1-overexpressing cancer cells. Bioorg Med Chem 23(15):4980–4988. https://doi.org/10.1016/j.bmc.2015.05.020
24. Kogias E, Osterberg N, Baumer B, Psarras N, Koentges C, Papazoglou A, Saavedra JE, Keefer LK, Weyerbrock A (2012) Growth-inhibitory and chemosensitizing effects of the glutathione-*S*-transferase-pi-activated nitric oxide donor PABA/NO in malignant gliomas. Int J Cancer 130(5):1184–1194. https://doi.org/10.1002/ijc.26106
25. Saunders IT, Mir H, Kapur N, Singh S (2019) Emodin inhibits colon cancer by altering BCL-2 family proteins and cell survival pathways. Cancer Cell Int 19:98. https://doi.org/10.1186/s12935-019-0820-3
26. Nishina A, Miura A, Goto M, Terakado K, Sato D, Kimura H, Hirai Y, Sato H, Phay N (2018) Mansonone E from *Mansonia gagei* inhibited alpha-MSH-induced melanogenesis in B16 cells by inhibiting CREB expression and phosphorylation in the PI3K/Akt pathway. Biol Pharm Bull 41(5):770–776. https://doi.org/10.1248/bpb.b17-01045
27. Spangle JM, Roberts TM (1868) Zhao JJ (2017) The emerging role of PI3K/AKT-mediated epigenetic regulation in cancer. Biochim Biophys Acta Rev Cancer 1:123–131. https://doi.org/10.1016/j.bbcan.2017.03.002
28. Ching CB, Hansel DE (2010) Expanding therapeutic targets in bladder cancer: the PI3K/Akt/mTOR pathway. Lab Invest 90(10):1406–1414. https://doi.org/10.1038/labinvest.2010.133
29. Matsuo FS, Andrade MF, Loyola AM, da Silva SJ, Silva MJB, Cardoso SV, de Faria PR (2018) Pathologic significance of AKT, mTOR, and GSK3beta proteins in oral squamous cell carcinoma-affected patients. Virchows Arch 472(6):983–997. https://doi.org/10.1007/s00428-018-2318-0
30. Butler DE, Marlein C, Walker HF, Frame FM, Mann VM, Simms MS, Davies BR, Collins AT, Maitland NJ (2017) Inhibition of the PI3K/AKT/mTOR pathway activates autophagy and compensatory Ras/Raf/MEK/ERK signalling in prostate cancer. Oncotarget 8(34):56698–56713. https://doi.org/10.18632/oncotarget.18082
31. Luo L, Zhao H, Luo Q (2018) Swerchirin exerts anticancer activity on SKOV3 human ovarian cancer cells via induction of mitochondrial apoptosis, G2/M cell cycle arrest and inhibition of Raf/MEK/ERK cascade. J BUON 23(1):111–116
32. Zhang Y, Li G, Liu X, Song Y, Xie J, Li G, Ren J, Wang H, Mou J, Dai J, Liu F, Guo L (2018) Sorafenib inhibited cell growth through the MEK/ERK signaling pathway in acute promyelocytic leukemia cells. Oncol Lett 15(4):5620–5626. https://doi.org/10.3892/ol.2018.8010
33. Morales-Ibanez O, Affo S, Rodrigo-Torres D, Blaya D, Millan C, Coll M, Perea L, Odena G, Knorpp T, Templin MF, Moreno M, Altamirano J, Miquel R, Arroyo V, Gines P, Caballeria J, Sancho-Bru P, Bataller R (2016) Kinase analysis in alcoholic hepatitis identifies p90RSK as a potential mediator of liver fibrogenesis. Gut 65(5):840–851. https://doi.org/10.1136/gutjnl-2014-307979
34. Kim HS, Kim SJ, Bae J, Wang Y, Park SY, Min YS, Je HD, Sohn UD (2016) The p90rsk-mediated signaling of ethanol-induced cell proliferation in HepG2 cell line. Korean J Physiol Pharmacol 20(6):595–603. https://doi.org/10.4196/kjpp.2016.20.6.595
35. Deliu IC, Neagoe CD, Bezna M, Genunche-Dumitrescu AV, Toma SC, Ungureanu BS, Uscatu CD, Bezna MC, Lungulescu CV, Padureanu V, Gheonea DI, Ciurea T, ForTofoiu M (2016) Correlations between endothelial cell markers CD31, CD34 and CD105 in colorectal carcinoma. Rom J Morphol Embryol 57(3):1025–1030
36. Toma SC, Uscatu CD, Ungureanu BS, Mirea CS, Dumitrescu T, Georgescu EF, Schenker M, Surlin V, Georgescu I (2018) Correlations between CD34 immunolabelled blood vessels and CD34 mRNA expression in colorectal cancer. Curr Health Sci J 44(1):60–63. https://doi.org/10.12865/CHSJ.44.01.10

37. Okkenhaug K, Graupera M, Vanhaesebroeck B (2016) Targeting PI3K in cancer: impact on tumor cells, their protective stroma, angiogenesis, and immunotherapy. Cancer Discov 6(10):1090–1105. https://doi.org/10.1158/2159-8290.CD-16-0716
38. Zhang C, Hao Y, Wu L, Dong X, Jiang N, Cong B, Liu J, Zhang W, Tang D, De Perrot M, Zhao X (2018) Curcumin induces apoptosis and inhibits angiogenesis in murine malignant mesothelioma. Int J Oncol 53(6):2531–2541. https://doi.org/10.3892/ijo.2018.4569
39. Liu L, Cao Y, Chen C, Zhang X, McNabola A, Wilkie D, Wilhelm S, Lynch M, Carter C (2006) Sorafenib blocks the RAF/MEK/ERK pathway, inhibits tumor angiogenesis, and induces tumor cell apoptosis in hepatocellular carcinoma model PLC/PRF/5. Cancer Res 66(24):11851–11858. https://doi.org/10.1158/0008-5472.CAN-06-1377